RELATIVE STABILITY OF CARBIDE AND INTERMETALLIC PHASES IN NICKEL-BASE SUPERALLOYS

H. E. Collins

Abstract

Twelve nickel-base superalloys were examined utilizing microscopy and residue analysis techniques to identify and to determine the relative stability for long times (up to 5000 hours) of gamma-prime and the minor phases in the 1400-2100°F temperature range. The materials studied included seven cast alloys, IN 100, B-1900, Inco 713C, MAR-M200, MAR-M246, TRW-NASA IVY and TRW-NASA VIA,and five wrought alloys, U-700, Rene' 41, Inconel 718, Waspaloy and Unitemp AF2-1D.

Seven minor phases were identified: MC, $M_{23}C_6$, M_6C, M_3B_2, sigma, mu and Ni_3Cb. MC was found in all twelve alloys; $M_{23}C_6$ in all alloys except TRW-NASA IVY and Inconel 718; M_6C in B-1900, MAR-M200, MAR-M246, TRW-NASA VIA, Rene' 41 and Unitemp AF2-1D; M_3B_2 in B-1900, Inco 713C, MAR-M200, MAR-M246, TRW-NASA IVY, TRW-NASA VIA and U-700; sigma in IN-100, Inco 713C, U-700, Rene'41 and Inconel 718; mu in Rene' 41 and Unitemp AF2-1D; and Ni_3Cb in Inconel 718. Complete solutioning of gamma-prime did not occur in the seven cast alloys even at the highest exposure temperature studied, 2100°F. Complete solutioning of gamma-prime occurred for the wrought alloys in the following temperature ranges: 1800-1900°F for Waspaloy, 1900-2000°F for Rene' 41 and 2000-2100°F for U-700 and Unitemp AF2-1D. Inconel 718 was an exception in that gamma-prime was not present at any of the temperatures studied after the long exposure times.

H. E. Collins is a Principal Engineer with the Materials Technology Laboratory, TRW Inc., Cleveland, Ohio 44117.

Introduction

In recent years, the success of the commercial airlines, coupled with the expanding needs for more and faster military aircraft, have provided the impetus for an increasing activity in propulsion system design and related material development. The immediate challenge for most of the current commercial and military aircraft power-plants has been met primarily through the use of nickel-base superalloys. These materials utilize three basic mechanisms for strengthening: intermetallic precipitation, solid solution and carbide precipitation. Unfortunately, two of the three mechanisms, intermetallic and carbide precipitation, are employed in a metastable condition. Hence, normal thermal exposures, such as experienced in processing, heat treatment or service, can alter the basic structure and distribution of these phases, thereby producing variations in the properties of the alloy. Thermal exposures also increase the possibility of further phase alterations, such as the formation of sigma, mu, eta, Laves or epsilon. Therefore, to utilize nickel-base superalloys effectively, e.g., in extending component service life reliability, it is necessary to have a thorough understanding of the phases present and to establish the effect of time, temperature and stress on these phases and on possible phase alterations.

The primary objective of this study was to identify and determine the relative stability for long times (up to 5000 hours) of gamma-prime and minor phases (e.g., carbides, borides, sigma, Laves, mu, epsilon). The alloys studied included five commonly used cast alloys, IN 100, B-1900, Inco 713C, MAR-M200 and MAR-M246; four commonly used wrought alloys, U-700, Rene'41, Inconel 718 and Waspaloy; two experimental NASA cast alloys, TRW-NASA IV Y and TRW-NASA VI A (1); and one experimental Air Force wrought alloy, Unitemp AF2-1D(2). The temperature range studied was from 1400°F to 2100°F.

Materials and Procedures

The twelve nickel-base superalloys selected for study in this investigation are given in Table I along with their chemical composition and electron-vacancy number Nv_{ss} (3).

A series of specimens were taken from each alloy, solution heat treated (wrought alloys only), and then aged in air for 5000 hours at temperatures between 1400 and 2000°F (100°F intervals) and for 2000 hours at 2100°F. No results were obtained for IN 100, MAR-M246 and Inconel 718 at 2100°F because of excessive oxidation of the specimens. The solutioning treatments are given in Table I. Metallographic and residue analysis techniques were then employed to evaluate the effects of the solutioning and aging treatments.

Metallographic examination included both light and electron microscopy. Specimens were prepared by mechanical polishing through 600-grit silicon carbide papers, followed by 20 and 40-grit carborundum papers. This was followed by polishing on billiard cloth and Syntron micro-cloth with aluminum oxide abrasive slurry. The final polishing operation was an electrolytic polishing consisting of 20 volts at 2.2 amps for approximately 3 seconds in a 15% sulfuric acid-methyl alcohol electrolyte. The specimens were then chemically etched with a 35% HCl (conc.)-ethyl alcohol solution with 4 drops of H_2O for each 5 ml of solution. Standard replication techniques utilizing collodion replicas shadowed with chromium and backed with carbon were employed for electron microscopy.

Residue analysis was employed to identify the minor phases. Specimens for this analysis were sandblasted and surface ground to remove surface contamination (e.g. oxides and nitrides) as a result of the heat treatment. The minor phases were extracted electrolytically from the alloy matrix in a 10% HCl-methanol solution. Five grams of tartaric acid per 100 ml of solution were added to retard the formation of tungstic acid during the extraction of the tungsten containing alloys. The digestion process generally varied from 16 to 24 hours with a current density of approximately 0.75 amps per sq. in. The residues were analyzed with a Norelco diffractometer using CuKα radiation and a nickel filter at a scanning speed of 1/2° per min. The diffraction patterns were then compared to known X-ray patterns in the ASTM card index or the published literature to identify the minor phases present in the residue. ASTM card number 6-0614 was utilized in identifying MC; card number 9-122 for $M_{23}C_6$; card number 11-546 for M_6C; card number 11-102 for mu; and card number 7-96 for sigma. Reference 4 was employed in identifying M_3B_2, and Reference 5 for Ni_3Cb.

Results

Minor Phase Results

Residue Analysis: The results showing the effects of the long time heat treatments on the concentrations of the minor phases are presented graphically in Figs. 1-12 for the twelve alloys studied. The values plotted on the ordinate are a semi-quantitative measure of the amount of the minor phases in the alloy (6). These results were derived from the intensity of the strongest X-ray line for each of the minor phases in conjunction with the amount of extracted residue. The rating scale can be interpreted roughly as follows: very abundant >1.2 wt.% of alloy, abundant ≈0.8 wt.%, medium ≈0.4 wt. %, rare ≈0.1 wt.% and very rare <0.05 wt.%. In addition, the lattice parameters of the minor phases identified in each alloy are given in Table 2.

The seven different minor phase types identified in the twelve nickel-base superalloys after the long time heat treatments were MC, $M_{23}C_6$, M_6C, M_3B_2, sigma, mu and Ni_3Cb. MC, the most prevalent of the seven minor phases, was found in significant concentrations in all twelve alloys. In addition, three of the alloys had more than one variety of MC present (i.e., different lattice parameters, Table 2). Inco 713C and TRW-NASA VI A each had two different varieties, while TRW-NASA IV Y had three. MC was generally stable and one of the more abundant phases only at the lower temperatures (e.g., 1400-1600°F) or at the higher temperatures (e.g., 2000-2100°F). MC became completely unstable in the temperature range 1700-1900°F in IN 100 (Fig. 1), 1700-2100°F in Inco 713C (Note that $MC_{(1)}$ became stable again near 2100°F while $MC_{(2)}$ did not, Fig. 3.) and 1600-1900°F in U-700 (Fig.8). The concentration of MC went through a minimum in the temperature range 1800-1900°F in B-1900 (Fig. 2), 1700-1900°F (trace amounts) in Rene' 41 (Fig. 9), 1700-1900°F in Inconel 718 (Fig. 10), 1500-1700°F (trace amounts) in Waspaloy (Fig. 11) and 1700-1900°F in Unitemp AF2-1D (Fig. 12). The amount of MC in MAR-M200 (Fig. 4) and MAR-M246 (Fig. 5) decreased with temperature above 1600°F until it reached a minimum (trace amounts) in the temperature range of 1800-2100°F for MAR-M200 and 1900-2000°F for MAR-M246. In TRW-NASA IV Y (Fig. 6) where three varieties of MC were found, $MC_{(1)}$ decreased with temperature above 1600°F until it reached a minimum in the 2000-2100°F temperature range; $MC_{(2)}$ increased with temperature above 1600°F until it reached a high in the 1900-2100°F temperature range; while $MC_{(3)}$ remained nearly constant until it became completely unstable above 1800-1900°F. In TRW-NASA VI A (Fig. 7) where two varieties of MC were found, $MC_{(1)}$ decreased with temperature above 1700°F, while $MC_{(2)}$ increased with temperature until it reached a maximum in the 2000-2100°F temperature range.

$M_{23}C_6$ was found in significant amounts in all alloys except TRW-NASA IVY and Inconel 718. It was generally stable only at lower temperatures, becoming completely unstable in the temperature range 1700-1800°F in B-1900, TRW-NASA VIA and Rene' 41; 1800-1900°F in MAR-M200, MAR-M246, Waspaloy and Unitemp AF2-1D; 1900-2000°F in U-700 and 2000-2100°F in IN 100 and Inco 713C. The maximum amount of $M_{23}C_6$, in general, occurred in the temperature range from about 1600 to about 1800°F.

M_6C was observed in significant amounts in B-1900, MAR-M200, MAR-M246, TRW-NASA VIA, Rene' 41 and Unitemp AF2-1D. It formed predominantly in the 1600-2000°F temperature range and became unstable above 2000°F in B-1900, TRW-NASA VIA, and Unitemp AF2-1D.

M_3B_2 was found in significant concentrations in B-1900, MAR-M246, TRW-NASA IVY, TRW-NASA VIA and U-700 and in trace concentrations in Inco 713C and MAR-M200. M_3B_2 was relatively stable in the temperature range 1700-1800°F in Inco 713C, MAR-M200, and MAR-M246; 1800-1900°F in TRW-NASA VIA; and 1900-2000°F in B-1900 and TRW-NASA IVY.

The minor intermetallic phases sigma and mu were observed in five alloys: IN 100, Inco 713C, U-700, Rene' 41 and Inconel 718. It was stable in the temperature range from 1400 to 1600-1700°F in IN 100 and Inco 713C, from 1400-1500 to 1600-1700°F in U-700, from 1400 to 1800-1900°F in Rene' 41 and 1400-1500°F in Inconel 718. The maximum amounts of sigma occurred in the vicinity of 1500°F for IN 100 and Inco 713C, 1600°F for U-700 and 1800°F for Rene'41. Mu was observed in Rene' 41 and Unitemp AF2-1D in the 1400 to 1700-1800°F temperature range.

Metallography Some of the minor phase morphologies found in these alloys are shown in Figs. 13 to 18. Two morphological forms of MC were identified. The usual massive type was found within the grains as well as in the grain boundaries in all twelve alloys. Examples of this type are shown in Figs. 13B, 14A, 15 and 17A. A script-like variety, shown in Fig. 15, was also noted in three heavily alloyed cast alloys containing large amounts of tungsten and tantalum, MAR-M246, TRW-NASA IVY and TRW-NASA VIA. This form was observed primarily in the low temperature range (i.e.,1400-1800°F).

$M_{23}C_6$ was observed principally in grain boundary areas. It was found in all alloys except TRW-NASA IVY and Inconel 718. In the wrought alloys, $M_{23}C_6$ was commonly seen as a continuous carbide film or platelet in the low temperature range; as shown in Figs. 14A and B and 17A. A second form which was observed in both cast and wrought alloys was the blocky particle lining the grain boundaries, as shown in Figs. 13D and 14C and D.

Two morphological forms of M_6C were also identified in this study. The more common morphology was the blocky particle which was commonly found in grain boundaries, Fig. 16A. This form was observed in all six M_6C containing alloys, B-1900, MAR-M200, MAR-M246, TRW-NASA VI A, Rene' 41 and Unitemp AF2-1D. The second type was the acicular or Widmanstatten form, shown in Figs. 16B and C. This particular morphology was observed only in the four cast alloys.

The phases, sigma, mu and Ni_3Cb (epsilon), were all observed in the same morphological form, an acicular or Widmanstatten pattern. Examples of sigma are presented in Figs. 13A-C and 14B, of mu in Fig. 17 and of Ni_3Cb in Fig. 18. Sigma was identified in five alloys, IN 100, Inco 713C, U-700, Rene' 41 and Inconel 718; mu in two alloys, Rene' 41 and Unitemp AF2-1D; and Ni_3Cb in one alloy, Inconel 718.

Gamma-Prime Results Gamma-prime formation and temperature of formation varied greatly depending upon the alloy content. The results, however, can generally be divided into two categories, the effects of the long time heat treatments upon gamma-prime in the heavily alloyed cast superalloys and their effects in the more dilute wrought superalloys.

The effect of the long time treatments on gamma-prime in the cast alloys are shown in Fig. 13 for IN 100. The long time treatments at 1400°F, Fig. 13A, appeared to have relatively little effect on the various gamma-prime types. That is, the eutectic; the coarse, somewhat blocky type of intragranular and the small, spherical second generation gamma-prime were virtually unchanged from that observed in the as-cast structure. Above 1400°F, Figs. 13B-F, the long time treatments caused the gamma-prime particles to agglomerate, with particle size increasing with temperature. In addition, envelopes of gamma-prime formed around the minor phase particles; and a continuous gamma-prime precipitate appeared in the grain boundaries. Above about 1800°F, the second generation gamma-prime solutioned along with some of the blocky gamma-prime. Some of the blocky gamma-prime remained even at the highest temperatures studied, Fig. 13F. Also note that small, spherical gamma-prime particles were observed in the microstructures of the high temperature specimens (above 1800°F), e.g., Fig. 13E. These particles resulted from the re-precipitation of the solutioned gamma-prime upon cooling and not from the heat treatment. The other cast alloys behaved in an analogous manner.

As in the case of the cast alloys, the gamma-prime particle size of the wrought alloys varied greatly with the heat treatment temperature. Examples of the gamma-prime morphologies observed in U-700 are presented in Fig. 14. Comparison of the gamma-prime particle size after the 1400°F treatment, Fig. 14A, with that of re-solutioned gamma-prime which re-precipitated upon cooling, Fig. 14E, indicated that the gamma-prime observed at 1400°F was probably formed during cooling. Thus, as with the cast alloys, the 1400°F heat treatment appeared to have little effect on gamma-prime. Above 1400°F, Figs. 14B-F, the size of the gamma-prime increased with increasing heat treatment temperature. The morphology also changed from the spherical particle to a coarse blocky particle. In addition, gamma-prime envelopes formed around the minor phase particles; and a continuous gamma-prime precipitate appeared in the grain boundaries. Gamma-prime began to resolution above 1800-1900°F. Above 2000-2100°F, gamma-prime went completely into solution.

The effects of the long time heat treatments on gamma-prime in Rene' 41, Waspaloy and Unitemp AF2-1D were similar to those for U-700. However, the temperature range for complete solutioning of the gamma-prime was lower for Rene' 41 and Waspaloy. The temperature range for complete solutioning of the gamma-prime was 1900-2000°F for Rene' 41 and 1800-1900°F for Waspaloy. These results are in agreement with those reported by Collins and Quigg (6) for U-700, Rene' 41 and Unitemp AF2-1D.

Inconel 718 was an exception to the other nickel-base superalloys in this study in that gamma-prime was not present at any of the temperatures studied after the long time heat treatments. The reason being that with the low aluminum and titanium content and the high columbium content, the gamma-prime has transformed into the orthorhombic epsilon phase Ni_3Cb.

Discussion

Some indication of the effect of long time heat treatments on the minor phases of the nickel-base alloys can be obtained by comparing these results (Figs. 1-12) with those previously reported by Collins and Quigg (6) (Figs. 19-23), who studied the effect of short time heat treatments (<100 hrs.) on five nickel-base alloys: IN 100, B-1900, U-700, Rene' 41 and Unitemp AF2-1D. Probably the most apparent effect of the long time heat treatments concerns the stability of the MC carbide, which is generally considered to be very stable and to be one of the most abundant of the minor phases in nickel-base alloys. The short time results of Collins and Quigg generally supported this conclusion. The results from the present study, however, clearly show that this is not true for long exposure times. MC was, in general, only stable and abundant at the lower temperatures (e.g., 1400-1600°F) where the rate of formation of $M_{23}C_6$ was low or at the higher temperatures (e.g., 2000-2100°F) where these phases were normally unstable. In addition, comparison of the MC and the $M_{23}C_6$ or M_6C results, Figs. 1-5, 7-9, 11 and 12, strongly suggests that MC (+gamma) was dissociating into $M_{23}C_6$ or M_6C (+ gamma-prime) in the intermediate temperature range (i.e., from about 1600 to about 2000°F). This phenomena was reported previously in B-1900, U-700, Rene' 41, U-500 and U-520 (6-9).

Comparison of the long and short time results also indicated that in IN 100 (Figs. 1 and 19), U-700 (Figs. 8 and 21), Rene' 41 (Figs. 9 and 22) and Unitemp AF2-1D (Figs. 12 and 23), the $M_{23}C_6$ content increased greatly for all temperatures where it was stable as a result of the longer exposure times. In addition, the upper limit of the $M_{23}C_6$ stability range was raised by about 100°F in IN 100 and was lowered by about 100°F in Rene' 41. In Unitemp AF2-1D, the lower limit of the $M_{23}C_6$ stability range was lowered from 1600-1700°F to 1400°F. $M_{23}C_6$ was also observed in B-1900 in the lower temperature range (1400 to 1700-1800°F) after long times. The M_6C content, like that of $M_{23}C_6$, increased greatly for all temperatures where it was stable in B-1900 (Figs. 2 and 20) and Unitemp AF2-1D and from 1600 to 1800-1900°F in Rene' 41. The results also indicated that M_3B_2 became unstable in IN 100 and the amount decreased for all temperatures in U-700. In addition, the long time treatments resulted in the stabilization of sigma in the 1400 to 1600-1700°F temperature range in IN 100 and the 1400-1500 to 1600-1700°F temperature range in Unitemp AF2-1D. In Rene' 41, the amount of mu and sigma increased greatly with time for all temperatures where they were stable. Also the upper limit of mu stability was lowered by approximately 100°F.

Some interesting observations can be made from the long time results with regards to the electron-vacancy number Nv_{ss} and some of the assumptions employed to compute such numbers. The electron-vacancy number Nv_{ss} (Table 1) predicted that of the twelve alloys studied only IN 100, U-700 and Unitemp AF2-1D were prone to sigma formation. The experimental results (Table 2 and Figs. 1-12) showed that sigma formed in IN 100 and U-700 but not in Unitemp AF2-1D where mu formed instead. In addition, Inco 713C, Rene' 41 and Inconel 718 formed sigma.

One of the assumptions normally made in computing such numbers is that M_6C will form in place of $M_{23}C_6$ when Mo + W $\geq$ 6.0 wt. %(10). An alternate criteria commonly used is that M_6C will form when Mo + 1/2 W $\geq$ 6.0 wt. %(3). The results indicated that these assumptions were in error on two accounts. First, comparison of the Mo and W contents with the minor phase results (Tables 1-2, Figs. 1-12) showed that six alloys had Mo + W $\geq$ 6.0 wt.% and that one of them, TRW-NASA IV Y, did not form M_6C. In addition, B-1900 with a Mo + W <6.0 wt.% did form M_6C. With regards to the alternate criteria, all alloys which fulfilled this condition did form M_6C; however, two alloys, B-1900 and TRW-NASA VIA, which did not fulfill the condition also formed M_6C. Second and more importantly, the results showed that all alloys which formed M_6C also formed $M_{23}C_6$ and that except for B-1900, $M_{23}C_6$ was more abundant than M_6C in the critical 1400 to 1600-1700°F temperature range where sigma generally forms. As a result, it would appear that unless an alloy is heat treated at a temperature high enough to make M_6C the more abundant phase (e.g., from about 1800°F to about 2000°F), only $M_{23}C_6$ should be considered in the calculation.

Another assumption generally made in computing electron-vacancy numbers is that one-half of the carbon forms MC and one-half forms either $M_{23}C_6$ or M_6C. The results while only semi-quantitative illustrated that this is generally not true. Not only does the ratio of carbon in the carbides vary from alloy to alloy but also with temperature in an alloy. In addition, two alloys, TRW-NASA IV Y and Inconel 718, formed only MC carbides. This situation was probably due to the high concentration of strong MC formers Ta, Cb and Hf in TRW-NASA IV Y and Cb in Inconel 718.

Fortunately, the error in the electron vacancy numbers resulting from errors in the type, amount and composition of the carbides is small, on the order of a few hundredths. However, such disparities strongly indicate the dangers of indiscriminately utilizing such calculations. They also indicate the need for additional knowledge concerning the types, amounts and compositions of the various phases in nickel-base alloys (particularly gamma-prime) and the Nv's of some of the elements, such as Mo and W, where there is some indication that the currently assigned values are incorrect (11).

The results of this study also offered some possible explanations for the deterioration of the mechanical properties with exposure time. For example, the continuous films or platelets of $M_{23}C_6$ in the grain boundaries (Figs. 14A and B and 17A) or the acicular or Widmanstatten pattern of M_6C, sigma, mu and Ni_3Cb provide easy pathways for crack propagation and thus can be deleterious to the properties of an alloy (3,12). In addition, the increase in the total concentration of minor phases in an alloy with time or the formation of new phases could possibly be detrimental to the properties by tying up the solid solution strengthening elements, such as Mo, W and Ta, so that they are no longer able to strengthen the alloy (9). Agglomeration of the various phases, particularly gamma-prime (Figs. 13 and 14) which is the major strengthener in nickel-base alloys (Ni_3Cb in Inconel 718), can also be very detrimental (3,9,12). It would appear from these results that in the case of the wrought alloys, it should be possible to provide some restoration of the mechanical properties of an alloy after long exposure by appropriate heat treatment. However, the inability to solution the gamma-prime before excessive grain growth or preferential liquation occurs severely limits the benefits from heat treatment of the cast superalloys.

Summary

Seven minor phases were identified in twelve nickel-base alloys after aging for 5000 hours in air at temperatures between 1400 and 2000°F and after 2000 hours at 2100°F. The phases were MC, $M_{23}C_6$, M_6C, M_3B_2, sigma, mu and Ni_3Cb. MC was found in all twelve alloys; $M_{23}C_6$ in all alloys except TRW-NASA IVY and Inconel 718; M_6C in B-1900, MAR-M200, MAR-M246, TRW-NASA VIA, Rene' 41 and Unitemp AF2-1D; M_3B_2 in B-1900, Inco 713C, MAR-M200, MAR-M246, TRW-NASA IVY, TRW-NASA VIA and U-700; sigma in IN 100, Inco 713C, U-700, Rene' 41 and Inconel 718; mu in Rene' 41 and Unitemp AF2-1D; and Ni_3Cb in Inconel 718. Complete solutioning of gamma-prime did not occur in the seven cast alloys even at the highest exposure temperature studied (2100°F). Complete solutioning of gamma-prime occurred for the wrought alloys in the following temperature ranges: 1800-1900°F for Waspaloy, 1900-2000°F for Rene' 41 and 2000-2100°F for U-700 and Unitemp AF2-1D. Inconel 718 was an exception in that gamma-prime was not present at any of the temperatures studied after the long exposure times.

The results indicated the following:

(1) MC was not completely stable in the intermediate temperature range (i.e., from about 1600 to about 2000°F) after long exposure times, but rather was dissociating into $M_{23}C_6$ or M_6C.

(2) Two assumptions concerning carbide formation which are normally employed to compute electron-vacancy numbers appeared to be incorrect. The results showed that the assumption that M_6C will form in place of $M_{23}C_6$ when Mo + W >6.0 wt.% (or the alternate criteria when Mo + 1/2 W >6.0 wt.%) was not valid. In addition, the assumption that one-half of the carbon was in MC and one-half in either $M_{23}C_6$ or M_6C was, in general, not true.

(3) The results also offered some possible explanations for deterioration of the mechanical properties with exposure time, including type, amount, morphology and agglomeration of the various phases.

Acknowledgements

The assistance of Mr. J. T. Laughlin in performing the experimental work and Messrs. W. J. Curtis and J. M. Dibee in performing the metallographic work is gratefully acknowledged.

References

1. H. E. Collins, "Development of High Temperature Nickel-Base Alloys for Jet Engine Turbine Buckel Applications," NASA Report CR-54507, TRW Inc. (June 20, 1967) Contract NAS3-7267.

2. F. J. Rizzo and L. W. Lherbier, "Research Directed Toward the Development of a Wrought Superalloy," Air Force Report AFML-TR-66-364, Universal-Cyclops Co. (November 1966) Contract AF33(615)-1729.

3. Chester T. Sims, "A Contemporary View of Nickel-Base Superalloys," Journal of Metals, 18 (October 1966) 1119.

4. H. J. Beattie, Jr., "The Crystal Structure of a M_3B_2 Type Double Boride," Acta Cryst, 11 (1958) 607.

5. M. Kaufman and A. E. Palty, "The Phase Structure of Inconel 718 and 702 Alloys," Trans. AIME 221 (1961) 1253.

6. H. E. Collins and R. J. Quigg, "Carbide and Intermetallic Instability in Advanced Nickel-Base Superalloys," ASM Trans. Quart., 61 (March 1968) 139.

7. W. P. Danesi, M. J. Donachie, and J. F. Radavich, "Phase Reactions in B-1900 Nickel-Base Alloy from 1600 to 1800°F," ASM Trans. Quart., 59 (1966) 505.

8. J. F. Radavich and W. J. Boesch, "A Study of Phase Reaction in a Complex 4.5 Al-3.5 Ti-Ni-Base Alloy," Advances in X-ray Analysis, Conference at Denver, Colorado (1960).

9. H. J. Murphy, C. T. Sims, and G. R. Heckman, "Long-Time Structures and Properties of Three High-Strength, Nickel-Base Alloys," Trans. AIME 239 (1967) 1961.

10. L. R. Woodyatt, C. T. Sims, and H. J. Beattie, Jr., "Prediction of Sigma-Type Phase Occurrence from Compositions in Austenitic Superalloys," Trans. AIME, 236 (1966) 519.

11. J. R. Mihalisin, C. G. Bieber, and R. T. Grant, "Sigma- Its Occurrence, Effect and Control in Nickel-Base Superalloys," Paper presented at the 1967 Annual AIME Meeting in Los Angeles, California.

12. C. P. Sullivan and M. J. Donachie, Jr., "Some Effects of Microstructure on the Mechanical Properties of Nickel-Base Superalloys," Metal Eng. Quart. (February 1967) 36.

Table 1. Nickel-Base Superalloys Evaluated

Alloy	Solutioning Treatment	C	Cr	Co	Mo	Ti	Al	W	B	Zr	Ta	Cb	Other
IN 100	As-cast	0.17	10.30	15.00	2.93	4.68	5.53	-	0.016	0.082	-	-	0.94V
B-1900	As-cast	0.10	8.25	9.50	5.89	1.07	5.98	-	0.016	0.10	4.19	-	-
Inco 713C	As-cast	0.12	13.25	-	4.28	0.81	6.40	-	0.009	0.05	-	2.66	-
MAR-M200	As-cast	0.14	9.51	10.3	-	2.06	5.05	12.15	0.010	0.048	-	0.99	-
MAR-M246 (Nominal)	As-cast	0.15	9.00	10.0	2.50	1.50	5.50	10.0	0.010	0.05	1.5	-	-
TRW-NASA IVY	As-cast	0.15	5.85	4.82	2.04	1.08	5.25	5.36	0.023	0.039	8.17	0.89	2.01Hf 0.90Re
TRW-NASA VIA	As-cast	0.16	6.03	7.19	2.24	0.98	5.26	5.78	0.018	0.12	8.32	0.34	0.46Hf 0.57Re
U-700	2150°F/4hr.	0.07	15.10	18.30	5.33	3.34	4.29	-	0.024	-	-	-	-
Rene' 41	2150°F/2hr.	0.08	19.31	10.82	9.77	3.23	1.51	-	0.006	-	-	-	2.34Fe
Inconel 718	1800°F/1hr.	0.06	18.86	-	2.99	0.93	0.57	-	-	-	-	5.25	17.48Fe
Waspaloy	1975°F/4hr.	0.06	19.30	14.60	4.39	3.08	1.42	-	-	0.051	-	-	-
Unitemp AF2-1D	2250°F/2hr.	0.33	11.93	14.20	5.05	3.04	4.60	4.93	0.014	0.10	1.48	-	-

* The alloy is considered to be sigma prone if Nv_{ss} >2.49 (9).

Table 2. Lattice Parameters of Minor Phases Identified by X-ray Diffraction of Extracte

Alloy	Phase, Å				
	$MC_{(1)}$	$M_{23}C_6$	M_6C	M_3B_2	Other
IN 100	4.34	10.78			Sigma - 8.83,4.58
B-1900	4.37	10.87	11.15	5.84,3.14	
Inco 713C	4.36	10.78		5.82,3.12	$MC_{(2)}$ - 4.47
					Sigma - 9.13,4.71
MAR-M200	4.34	10.80	11.17	N.D.**	
MAR-M246	4.37	10.85	11.25	5.83,3.18	
TRW-NASA IVY	4.44			5.83,3.14	$MC_{(2)}$ - 4.56
					$MC_{(2)}$ - 4.53
TRW-NASA VIA	4.42	10.77	11.21	5.83,3.19	$MC_{(3)}$ - 4.48
U-700	4.34	10.80		5.80,3.14	Sigma - 9.00,4.67
Rene' 41	4.33	10.82	11.19		Mu - 4.80,25.86
					Sigma - 9.20,4.76
Inconel 718	4.47				Ni_3Cb - 5.20,4.30,
					Sigma - 8.96, 4.63
Waspaloy	4.34	10.73			
Unitemp AF2-1D	4.35	10.79	11.23		Mu - 4.78, 25.7

* Residues extracted electrolytically in a 10% HCl-methanol solution.

** Not determined.

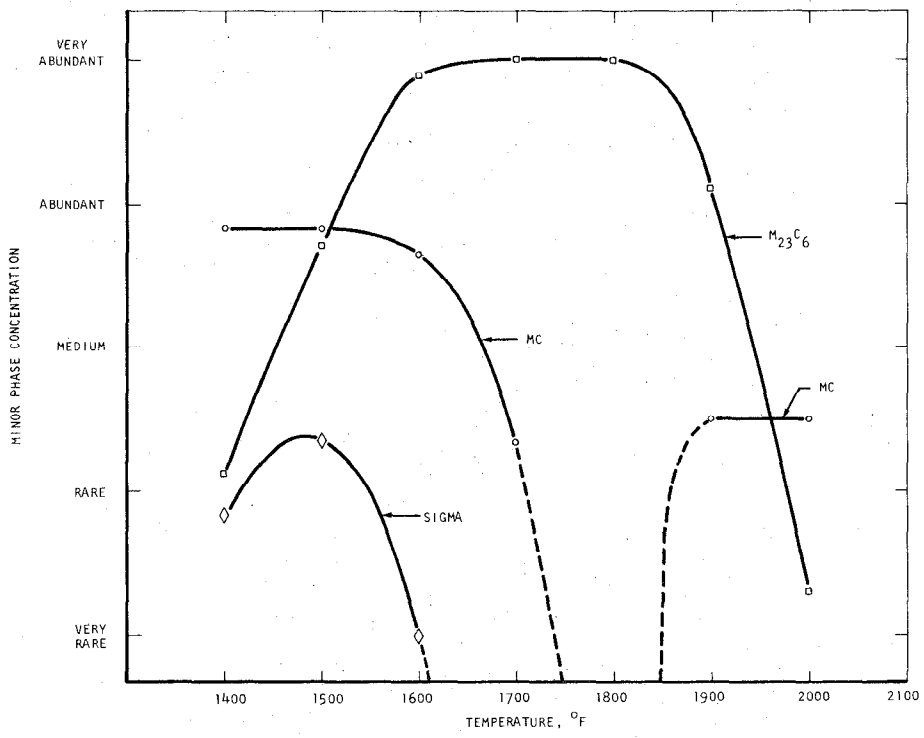

Figure 1. Minor phase concentration in IN-100 as a function of temperature for long exposure times.

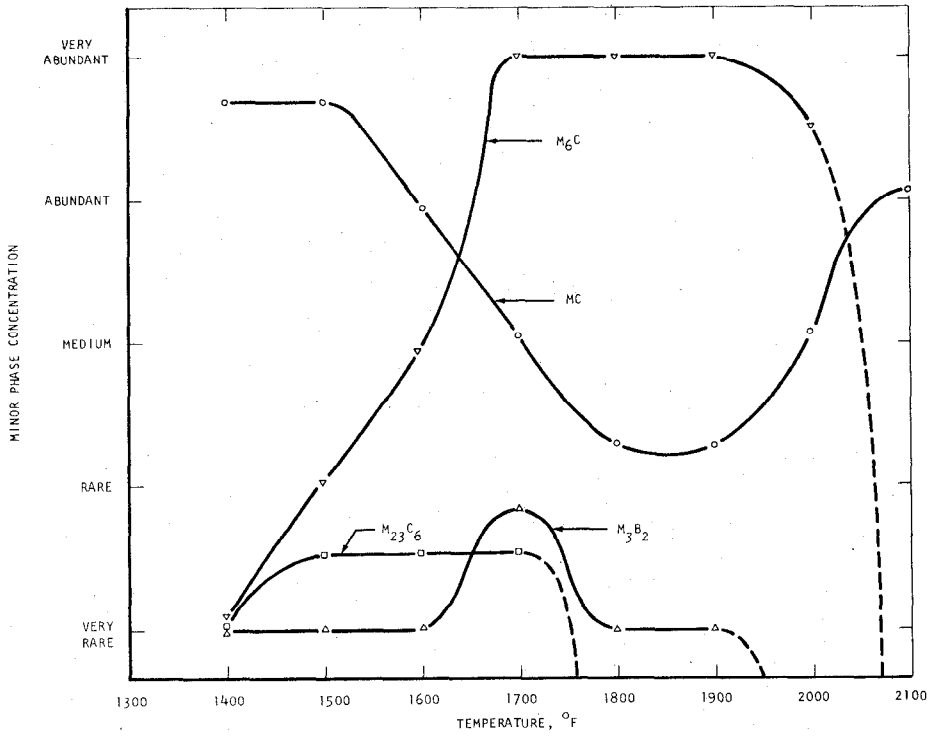

Figure 2. Minor phase concentration in B-1900 as a function of temperature for long exposure times.

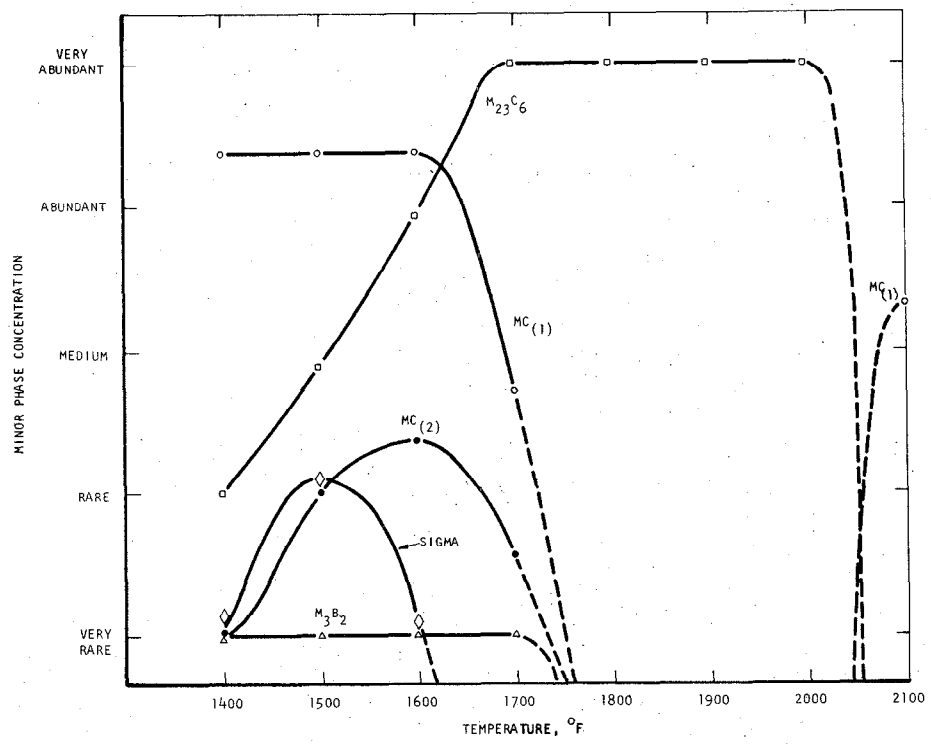

Figure 3. Minor phase concentration in Inco 713C as a function of temperature for long exposure times.

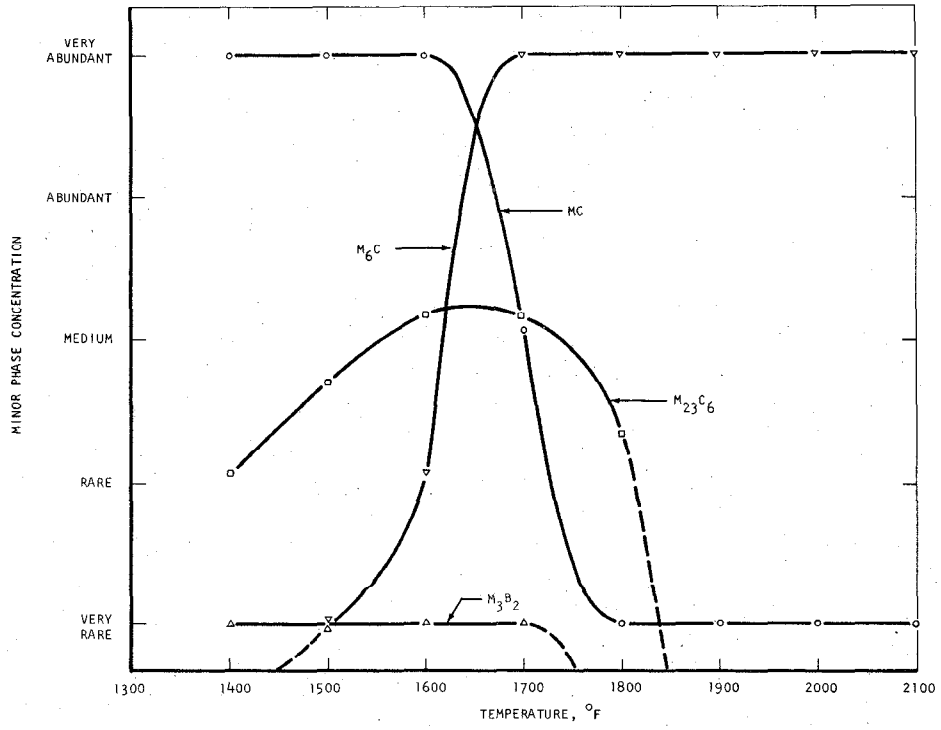

Figure 4. Minor phase concentration in MAR-M200 as a function of temperature for long exposure times.

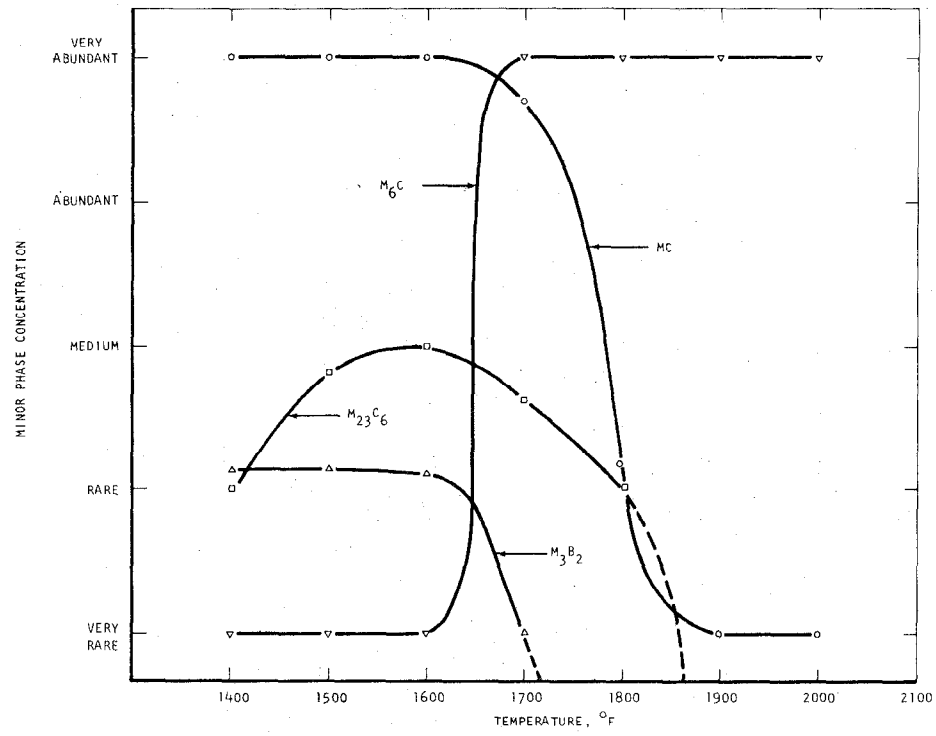

Figure 5. Minor phase concentration in MAR-M246 as a function of temperature for long exposure times.

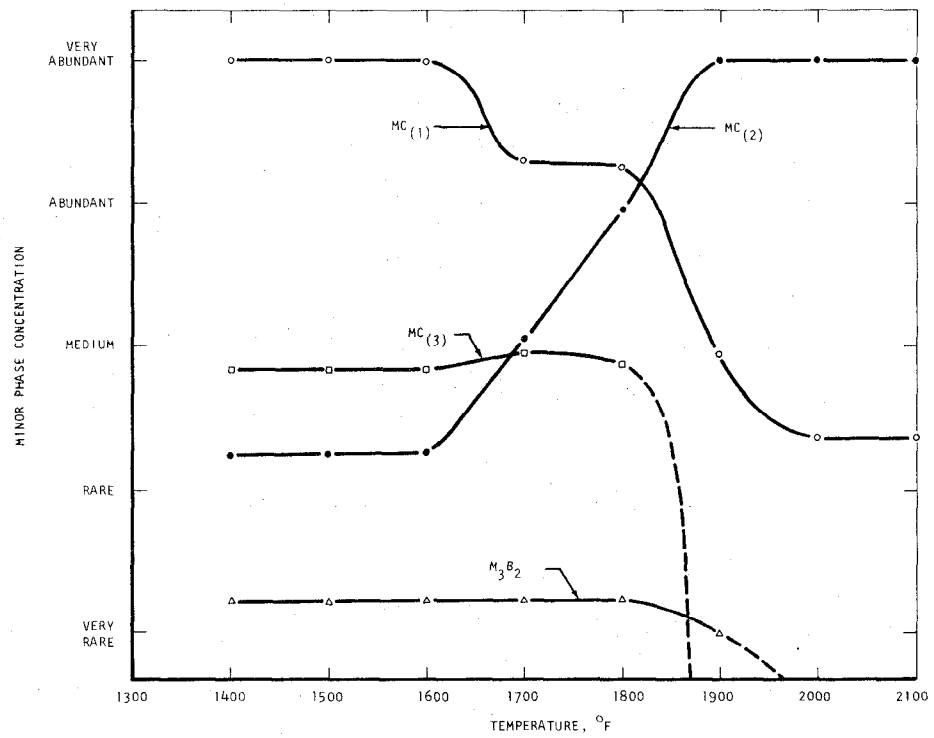

Figure 6. Minor phase concentration in TRW-NASA IVY as a function of temperature for long exposure times.

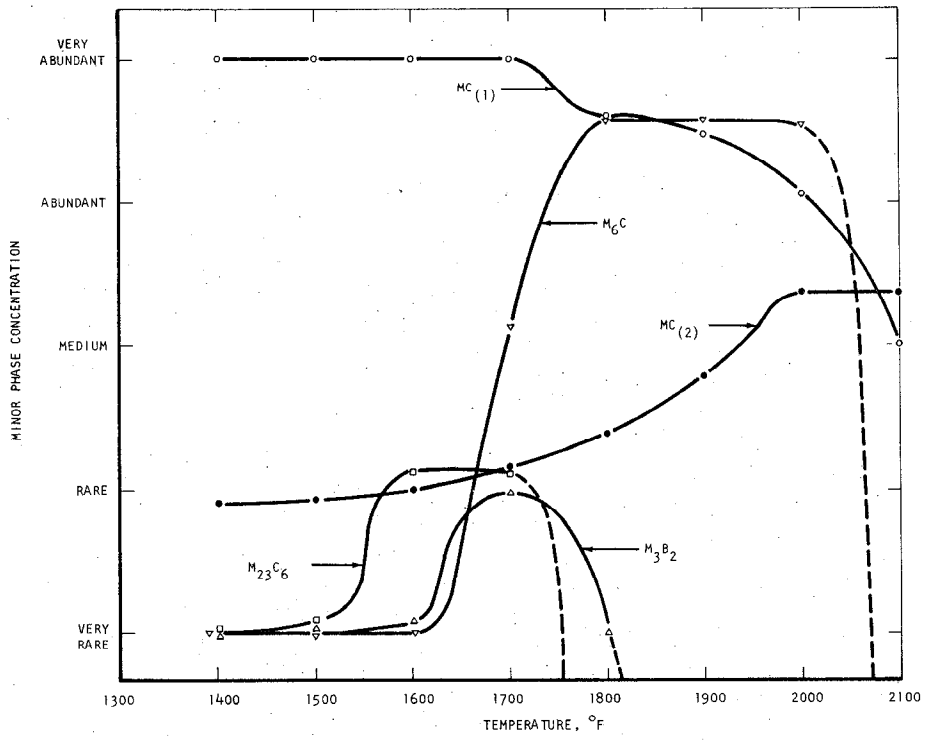

Figure 7. Minor phase concentrations in TRW-NASA VIA as a function of temperature for long exposure times.

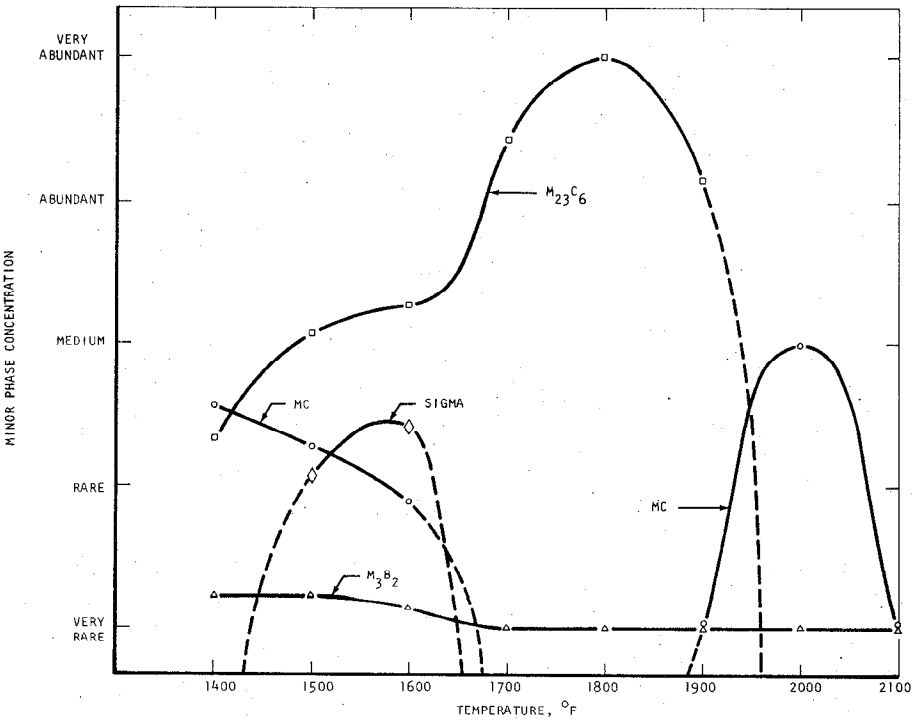

Figure 8. Minor phase concentration in U-700 as a function of temperature for long exposure times.

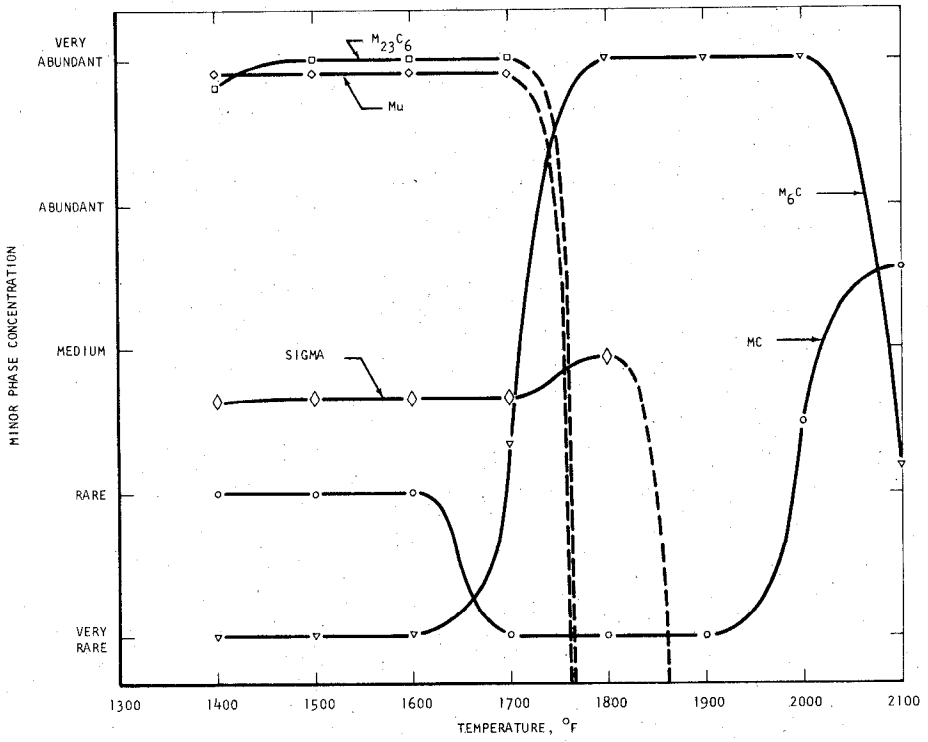

Figure 9. Minor phase concentration in Rene' 41 as a function of temperature for long exposure times.

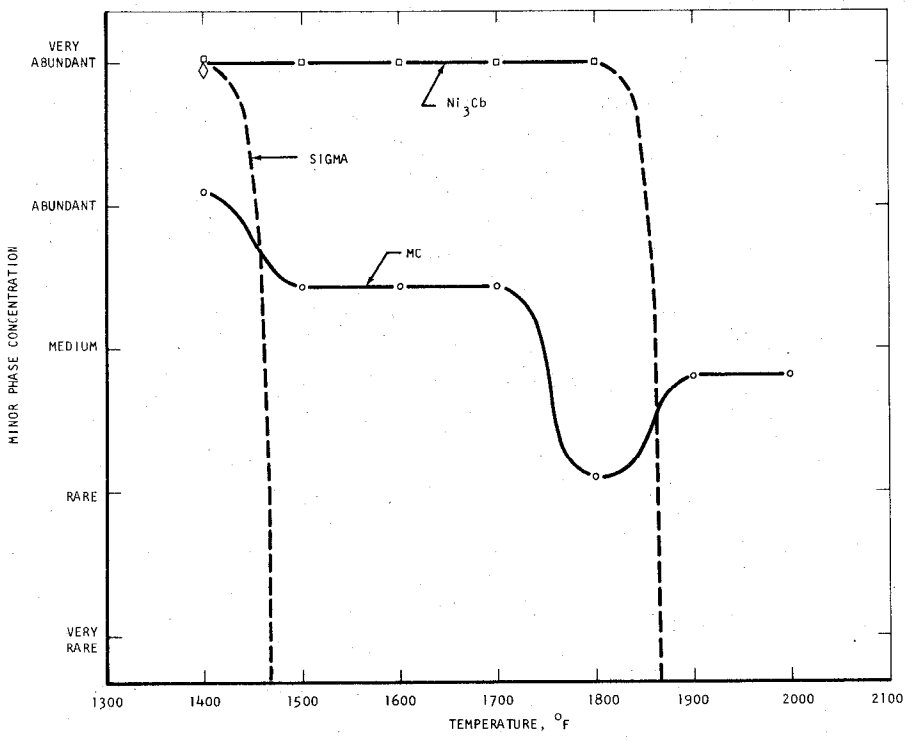

Figure 10. Minor phase concentration in Inconel 718 as a function of temperature for long exposure times.

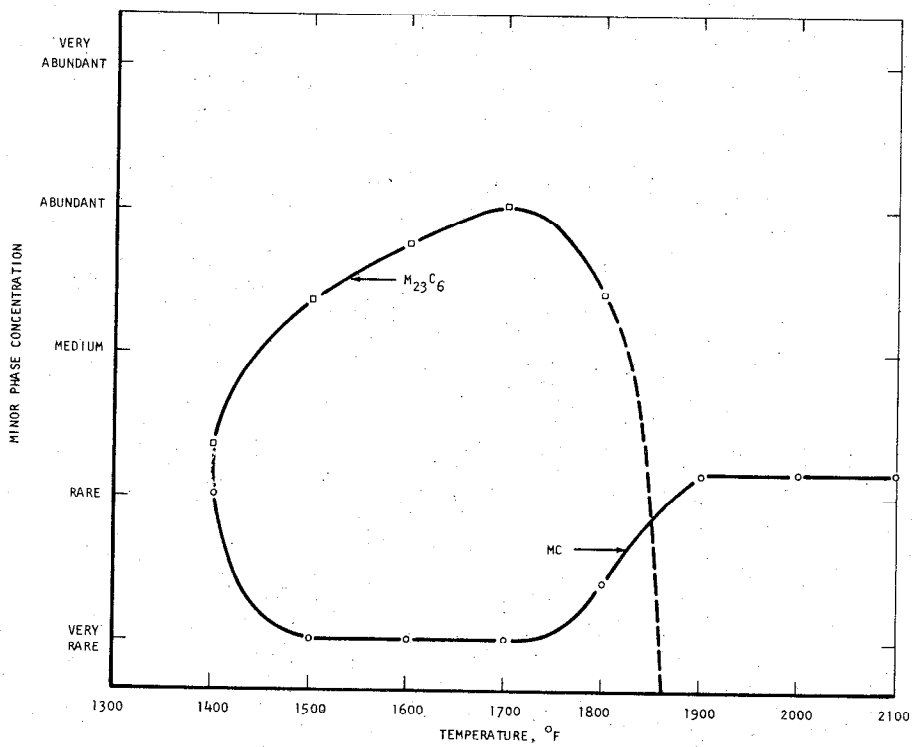

Figure 11. Minor phase concentration in Waspaloy as a function of temperature for long exposure times.

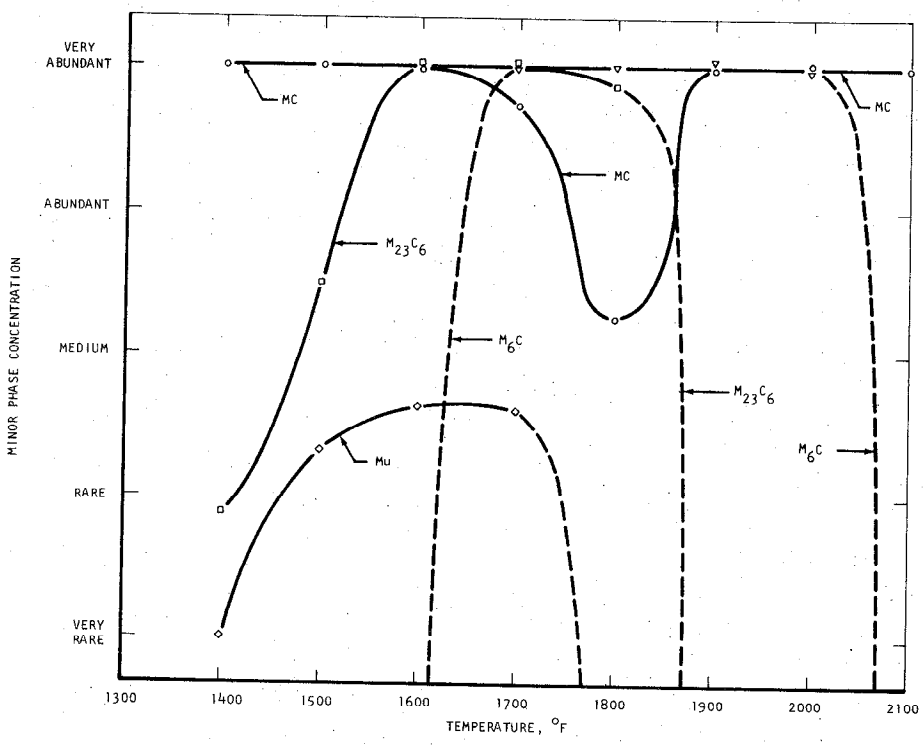

Figure 12. Minor phase concentration in Unitemp AF2-1D as a function of temperature for long exposure times.

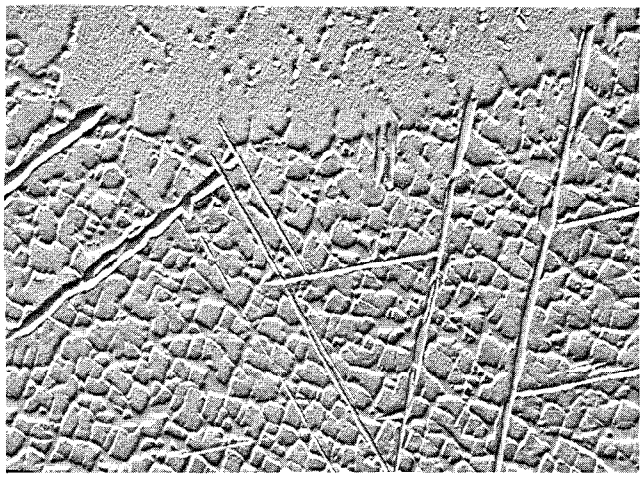

A) Electron micrograph showing gamma-prime and sigma (acicular phase) at 1400°F/5000 hrs. X6000.

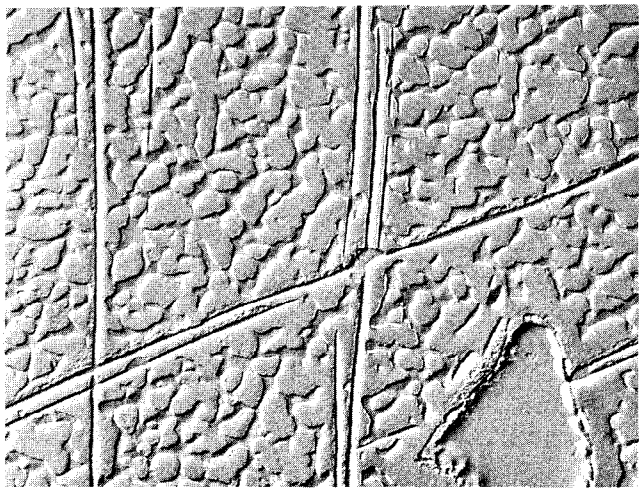

B) Electron micrograph showing gamma-prime, sigma and massive MC at 1500°F/5000 hrs. X6000.

Figure 13. Examples of the effect of long time heat treatments on the microstructure of IN 100.

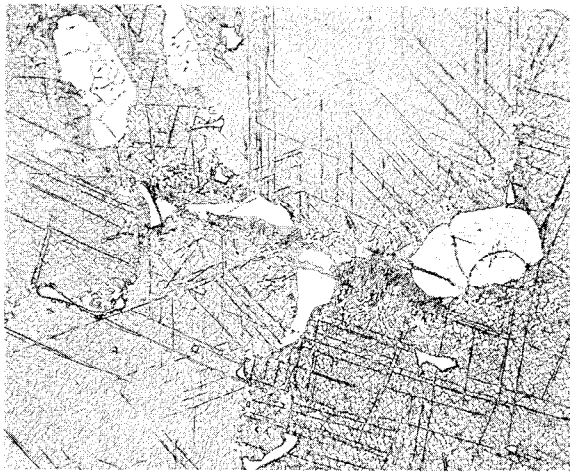

C) Light micrograph showing gamma-prime, sigma and massive MC at 1500°F/5000 hrs. X500.

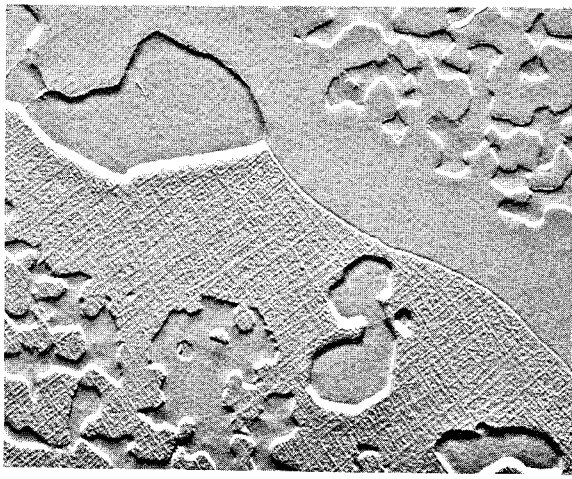

D) Electron micrograph showing gamma-prime and $M_{23}C_6$ in grain boundary at 1700°F/5000 hrs. X6000.

Figure 13 (continued) Examples of the effect of long ti treatments on the microstructure of IN-100.

Reduce 30% for publication

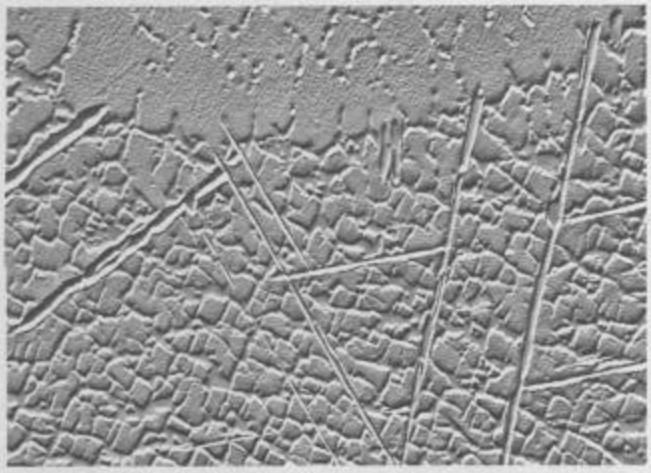

A) Electron micrograph showing gamma-prime and sigma (acicular phase) at 1400°F/5000 hrs. X6000.

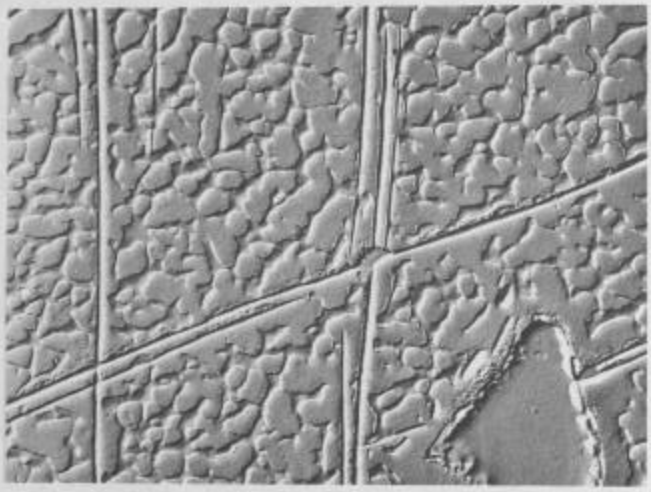

B) Electron micrograph showing gamma-prime, sigma and massive MC at 1500°F/5000 hrs. X6000.

Figure 13. Examples of the effect of long time heat treatments on the microstructure of IN 100.

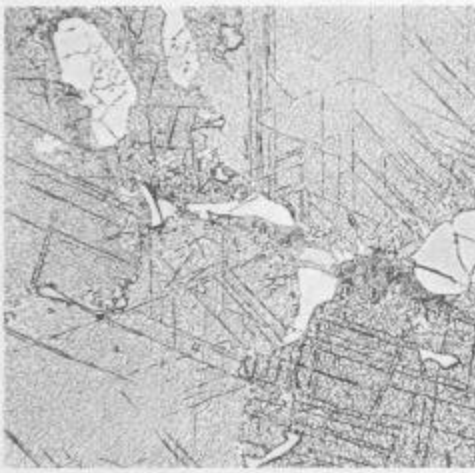

C) Light micrograph showing gamma-prime, massive MC at 1500°F/5000 hrs. X500.

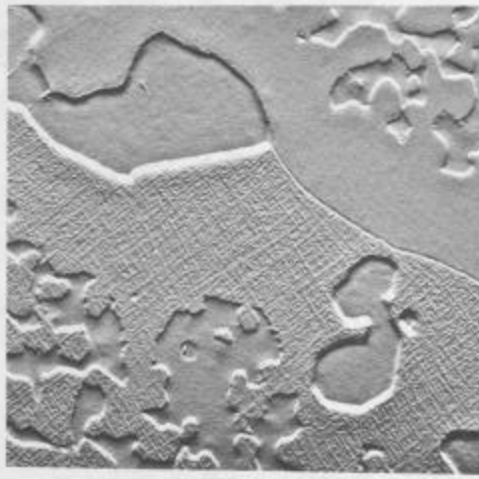

D) Electron micrograph showing gamma-prime in grain boundary at 1700°F/5000 hrs.

Figure 13 (continued) Examples of the effect o treatments on the microstructure of I

Reduce 30% for publication

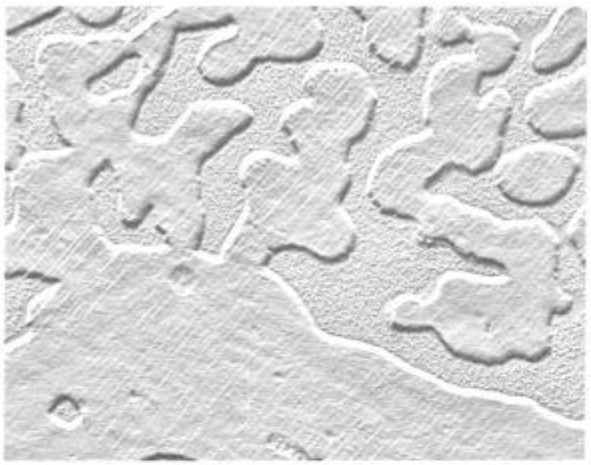

E) Electron micrograph showing gamma-prime at 1900°F/5000 hrs. X 6000.

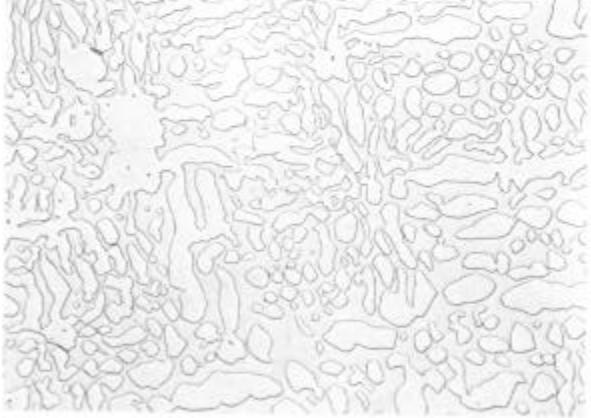

F) Light micrograph showing gamma-prime at 2000°F/5000 hrs. X500.

Figure 13 (continued) Examples of the effect of long time heat treatments on the microstructure of IN-100.

A) Electron micrograph showing gamma-prime, ma
MC and grain boundary $M_{23}C_6$ at 1400°F/5000

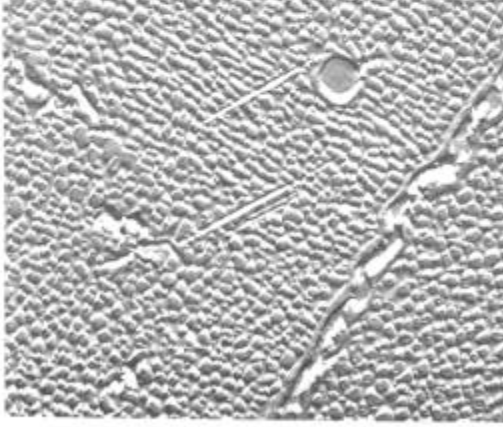

B) Electron micrograph showing gamma-prime, g
$M_{23}C_6$ and sigma at 1500°F/5000 hrs. X6000

Figure 14. Examples of the effect of long time hea
the microstructure of U-700.

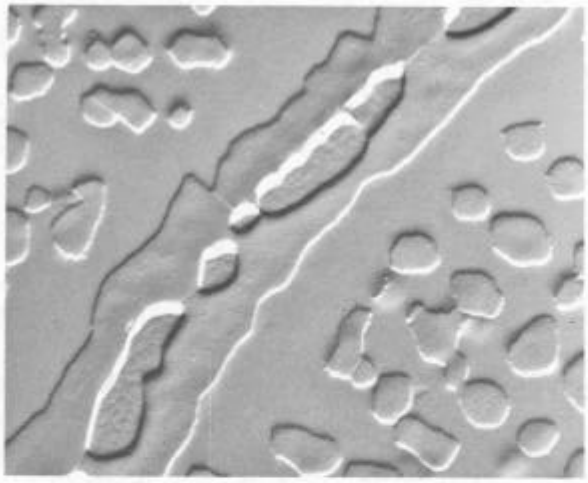

C) Electron micrograph showing gamma-prime and $M_{23}C_6$ in grain boundary at 1800°F/5000 hrs. X6000.

D) Light micrograph showing gamma-prime and $M_{23}C_6$ in grain boundaries at 1800°F/5000 hrs. X500.

Figure 14 (continued) Examples of the effect of long time heat treatments on the microstructure of U-700.

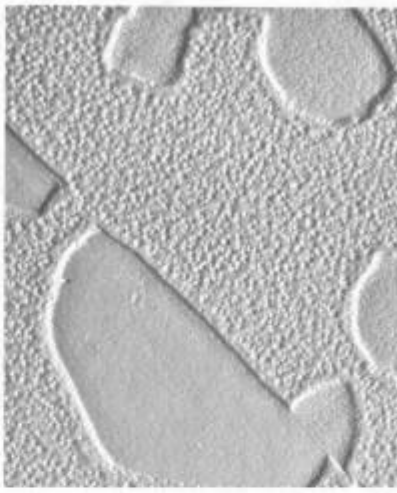

E) Electron micrograph showing gamma-pri
X6000.

F) Light micrograph showing gamma-prime
X500.

Figure 14 (Continued) Examples of the ef
treatments on the microstructur

Reduce 30% for publication

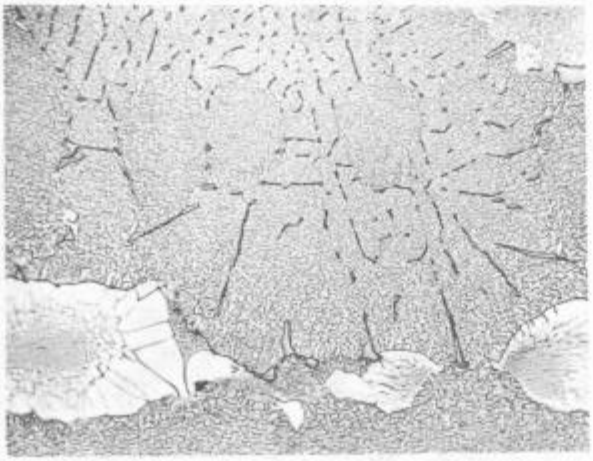

Figure 15. Light micrograph showing massive and script-like MC in TRW-NASA VIA. X500.

A) Electron micrograph showing blocky M_6C particles in grain boundary of Unitemp AF2-1D at 1900°F/5000 hrs. X6000.

Figure 16. Examples of M_6C morphologies.

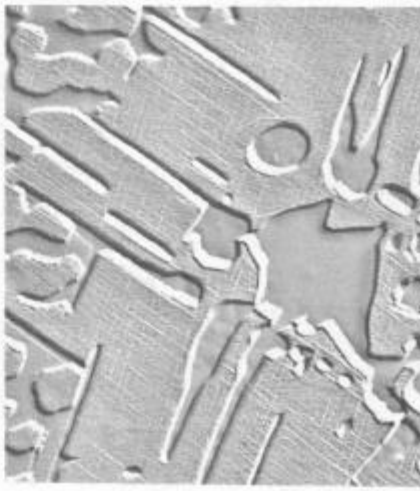

B) Electron micrograph showing acicula at 1800°F/5000 hrs. X6000.

C) Light micrograph showing acicular at 1800°F/5000 hrs. X500.

Figure 16. (Continued) Examples of M

Reduce 30% for publication

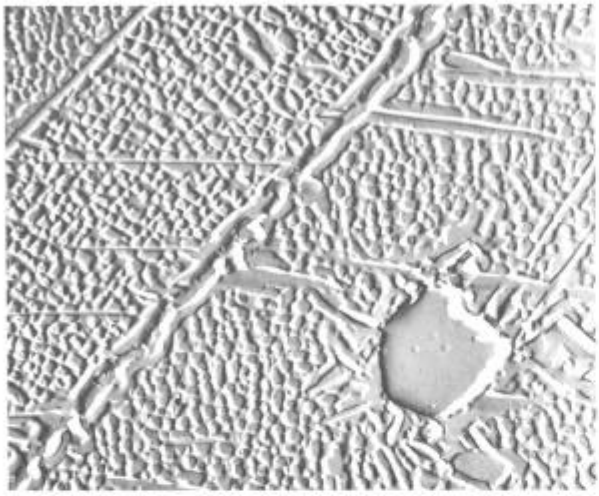

A) X6000.

B) X500.

Figure 17. Micrographs showing mu (acicular phase), grain boundary $M_{23}C_6$ and massive MC in Unitemp AF2-1D at 1500°F/5000 hrs.

A) 1600°F/5000 hrs. X60

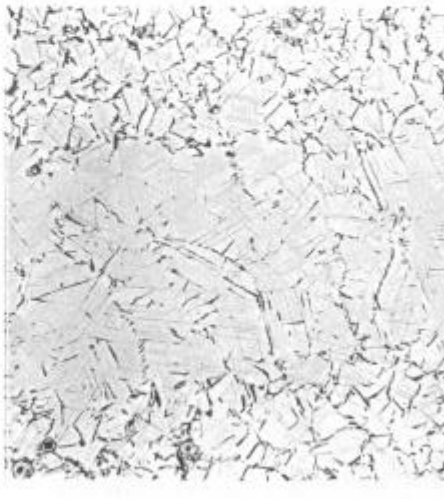

B) 1400°F/5000 hrs. X5

Figure 18. Micrographs showing Ni_3Cb i

Reduce 30% for publication

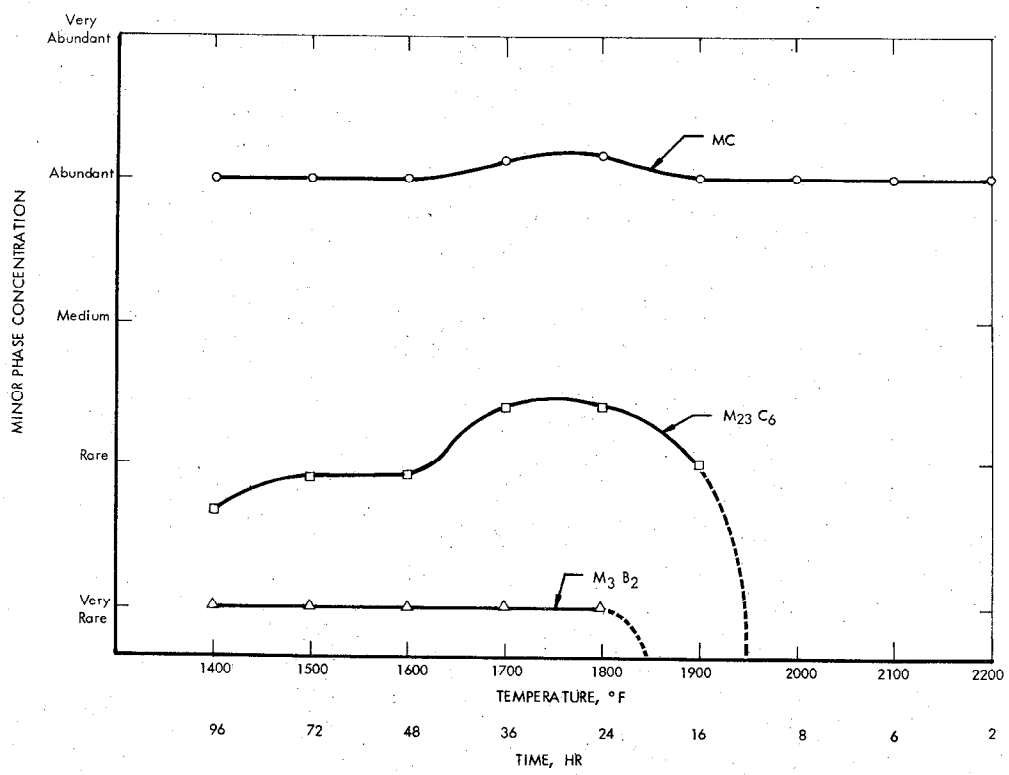

Figure 19. Minor phase concentration in IN 100 as a function of temperature for short exposure times from Collins and Quigg (6).

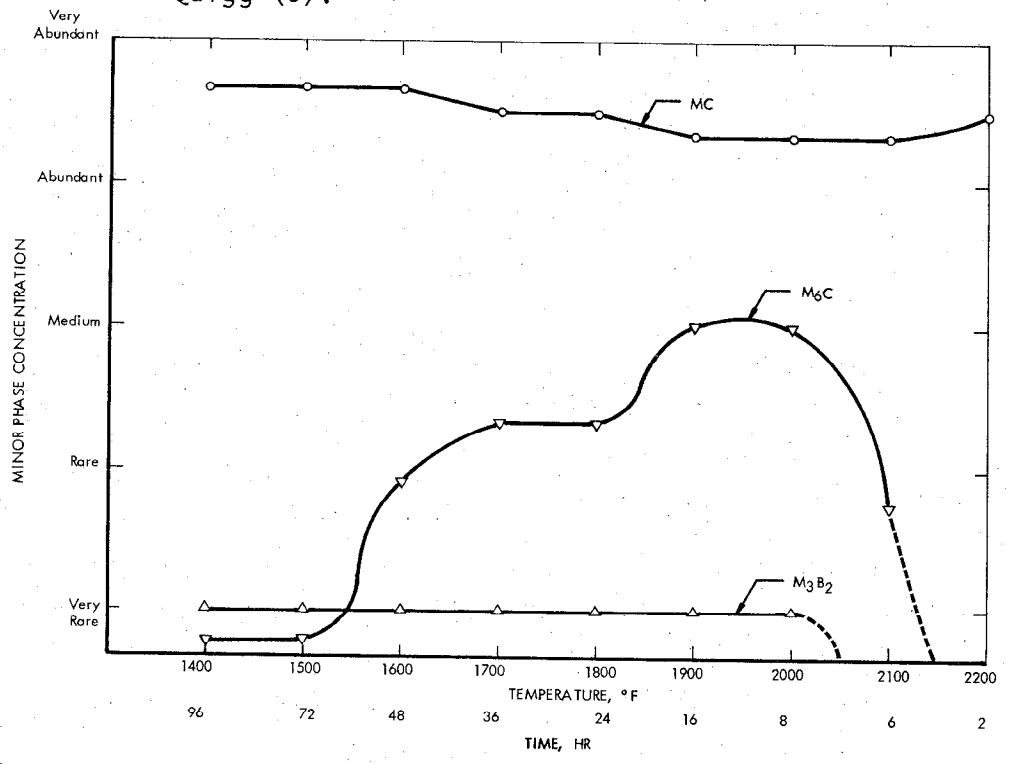

Figure 20. Minor phase concentration in B-1900 as a function of temperature for short exposure times from Collins and Quigg (6).

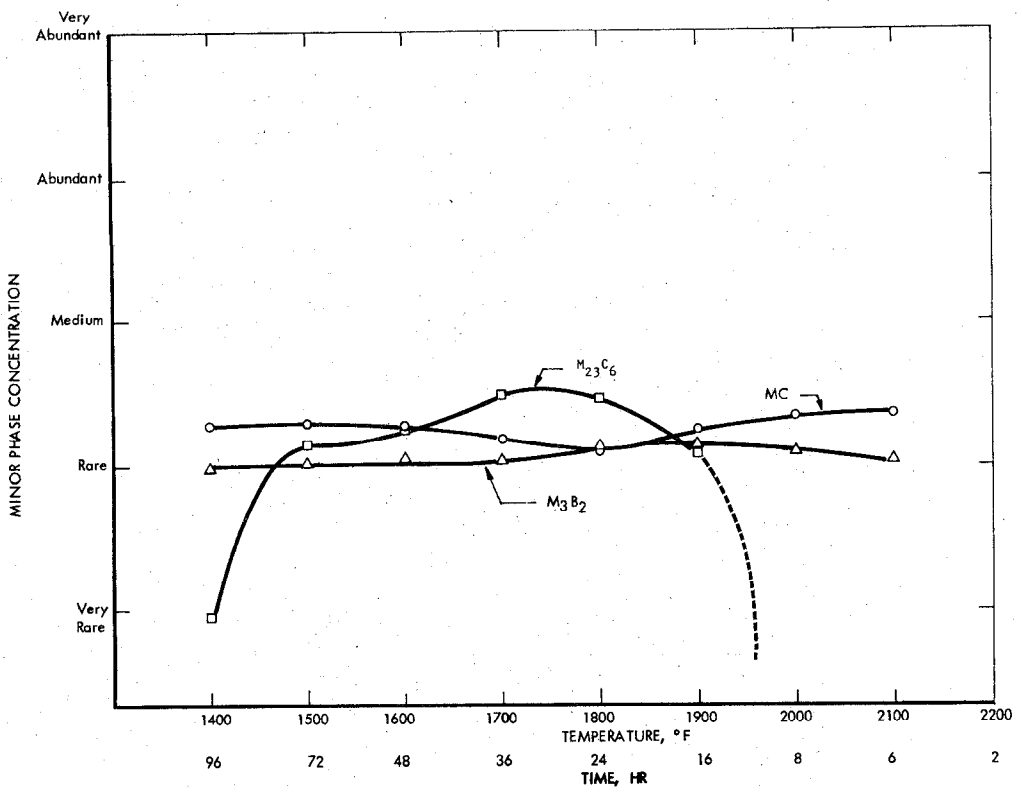

Figure 21. Minor phase concentration in U-700 as a function of temperature for short exposure times from Collins and Quigg (6).

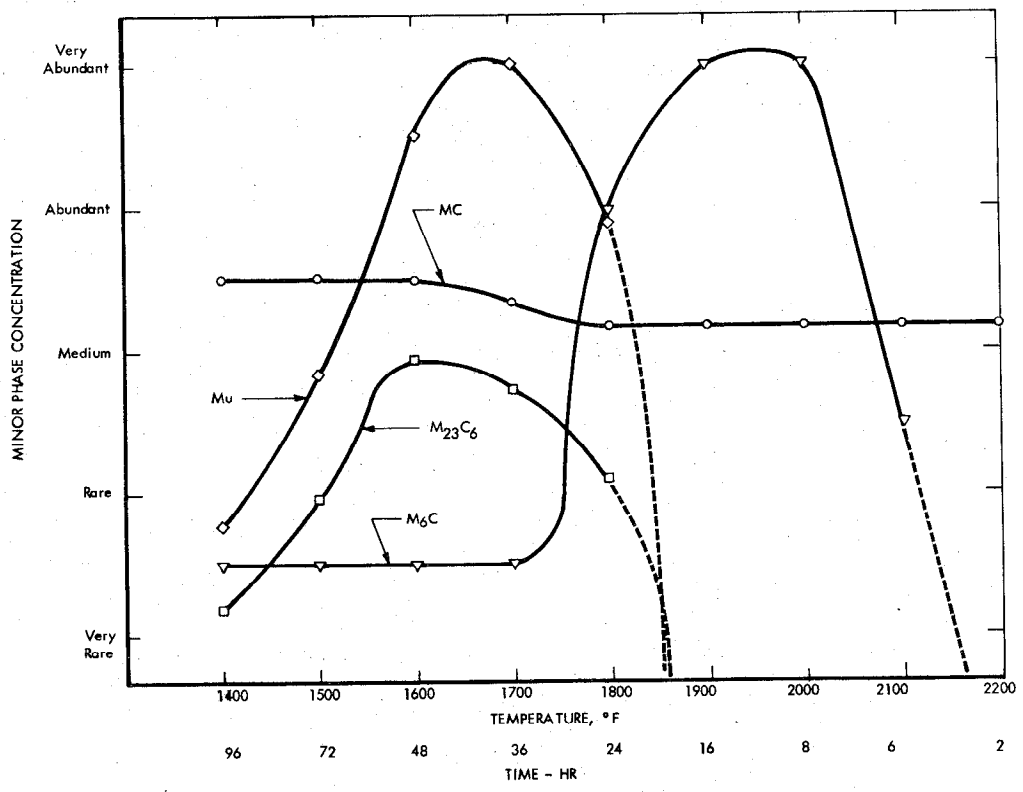

Figure 22. Minor phase concentration in Rene' 41 as a function of temperature for short exposure times from Collins and Quigg (6).

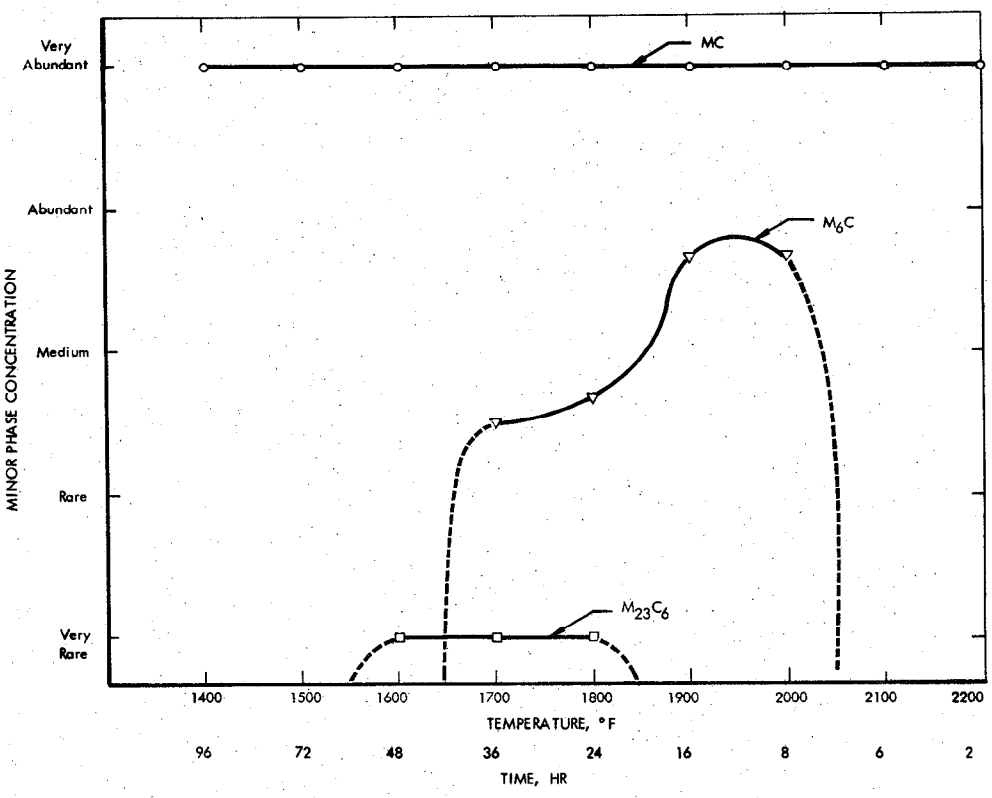

Figure 23. Minor phase concentration in Unitemp AF2-1D as a function of temperature for short exposure times from Collins and Quigg (6).